

## Investigation of Effect of Nozzle Geometry on Spray Characteristics with a 3D Eulerian Spray Model Coupled with the Nozzle Cavitating Flow

Zhaochen Jiang, Zhixia He<sup>\*</sup>, Qian Wang, Juyan Liu, Wenjun Zhong  
School of energy and power engineering, Jiangsu university, China

### Abstract

It is well known that near-nozzle fuel liquid jet development dominated by internal nozzle flow and fluid-dynamic instability governs the primary break-up process of the injected fuel. The fuel primary atomization controls the mixing of fuel with surrounding oxidant gas, which is significant to achieve highly-efficient and clean combustion for diesel engines. Different nozzle geometries under the same working conditions can lead to dramatically different behaviors in combustion performance and emissions formation. While the relation between nozzle flow and spray development in the combustion chamber is still a challenging topic with a high improvement potential. Based on the third-generation synchrotrons of Shanghai synchrotron radiation facility (SSRF), the high-precision three-dimension structure of nozzle with detailed internal geometry information were obtained, which is the basis of the subsequent numerical simulation. A 3D-Eulerian Spray multiphase model coupled with the cavitating flow inside the nozzle was put forward to simulate the whole spray process, including the primary atomization and secondary break-up. The nozzle flow and near-field spray were simulated with the VOF multiphase model. At a certain downstream location, where the spray is diluted, this Eulerian spray approach was switched to conventional Lagrangian approach. In this model, the fuel volume fraction of the cell at the switch position determined the droplet size. This entire methodology was validated through the experimental data of liquid spray penetration under non-evaporating chamber conditions. The multi-scheme numerical simulations were carried out by this model to investigate effect of the nozzle geometry and configuration on inner cavitating flow and the subsequent spray characteristics.

**Key Words** : diesel engine; nozzle; X-rays; cavitating flow; primary atomization; spray model

---

### Introduction

High-pressure diesel injection is an enabling technology for modern low-emission and high-efficiency diesel engines. But the atomization mechanisms for high-speed liquid jets are still not well understood and knowledge is incomplete, even after more than one hundred years of study, both experimentally and numerically. For a typical spray in diesel engines, spray tip penetration, spray angle, droplet size and number density and their distributions have been the primary interests of investigations. With the advent of advanced experimental techniques, it is now possible to obtain more detailed spray information, such as the fine spray structure, spray momentum, and liquid volume (or mass) fraction distributions. All these efforts have provided and will continue to provide new insights and motivations for the development of new spray atomization models<sup>[1]</sup>.

Cavitation and turbulence inside a diesel injector play a critical role in primary spray breakup and development processes. In diesel fuel injectors, cavitation can be beneficial to the development of the fuel spray, since the primary atomization and subsequent break-up of the liquid fuel jet can be enhanced. Primary breakup is believed to occur in the region very close to the nozzle tip as a result of turbulence, aerodynamics, and inherent instability caused by the cavitation patterns inside the injector nozzle orifices. In addition, cavitation enhances the liquid velocity at the nozzle exit due to the reduced exit area available for the liquid. Cavitation patterns extend from their starting point around the nozzle orifice inlet to the exit, where they influence the formation of the emerging spray. Geometrical parameters include the type of sac volume (valve covered orifice VCO, IMPROVED or miniSAC), orifice inlet curvature, orifice length, ratio of inlet to outlet orifice diameter, and its surface roughness. Dynamic parameters include the imposed pressure gradient, injector needle lift, and needle eccentricity. The study of cavitation in realistic injectors is challenging, both theoretically and experimentally, since the associated two-phase flow field is turbulent and highly complex, characterized by large pressure gradients and small orifice geometries<sup>[2-5]</sup>.

It is rather difficult to obtain the internal accurate three-dimensional geometric structure by non-destructive traditional methods due to the structural characteristics of the diesel fuel injector nozzles. The problem can be solved effectively by the use of synchrotron radiation technology<sup>[6]</sup>. The precise nozzle geometrical parameters provide a reliable basis for the numerical simulation of the whole flow and subsequent spray process simulation.

---

<sup>\*</sup>Corresponding author: [zxhe@ujs.edu.cn](mailto:zxhe@ujs.edu.cn) (Zhixia He)

The most efficient and widely-applied approach is the Lagrangian-Droplet-Eulerian-Fluid (LDEF) method, as can be seen in many commercial software and open source codes. Instead of solving the liquid phase as a partial-differential-equation based continuum such as in, the LDEF method treats the liquid as discrete particles. These particles are assumed to be negligible in volume and are superimposed on the continuous gas phase as material points. At the nozzle exit, liquid fuel is injected as discrete “blobs”, and a linear stability based phenomenological model is applied to account for the primary breakup [7-8]. In spite of its efficiency, the accuracy in the near-nozzle region is low, due to fact that the liquid fuel is actually a continuum as observed in both experiments and DNS. As a result, the model's connection to the nozzle flow is inherently weak, despite some efforts to model the unresolved near-nozzle physics and to consider the effects of in-nozzle cavitation and turbulence on the primary breakup [9-10].

In this paper, the accurate three-dimensional geometric structure of the real nozzle was measured as a basis for numerical simulations. In STAR-CD software, VOF method was used to simulate the internal nozzle flow and the original position of the traditional LDEF method was set in the dilute spray region of the nozzle downstream, thus nozzle flow (cavitation and turbulence) and the efforts of aerodynamics in the dense region commonly influencing of primary atomization could be considered comprehensively. The velocity (magnitude and direction) and density of the upstream Euler flow were made as the initial conditions of the downstream LDEF and then the spray angle and spray penetration of the diesel spray were simulated effectively, reflecting the asymmetric properties caused by turbulence and cavitation. At present, the initial parcel size in the simulation is given by empirical formula. Then, in order to validate this simulation model, comparisons with experimental data were performed. Finally, Effect of different injector geometries on the spray angle, penetration, and particle size distribution under different injection pressures were investigated.

### Synchrotron Radiation Measurement of Nozzle Structure

Synchrotron radiation is the electromagnetic radiation generated by electronic which changes direction in curvilinear motion at nearly the speed of light in a magnetic field. Synchrotron Radiation is greatly distinguished from conventional light. Synchrotron radiation is characterized by unparalleled functions: high collimation, high polarization, high coherence, wide spectral range, high spectrum, high photon flux and so on. Shanghai Synchrotron Radiation Facility (SSRF) is a third-generation synchrotron radiation facility which can provide a variety of synchrotron radiation from infrared light to hard X-ray [11].

As shown in figure 1, the experiment was made on the X-ray imaging and biomedical applications beam line station BL13W1 (SSRF). The station employed Wiggler light which can adjust photon energy ranging from 8~72.5keV, energy resolution less than  $3 \times 10^{-3}$ , maximum beam size 48mm(H) $\times$ 5.3mm(V), photon flux density  $1.9 \times 10^{10}$ phs/s/mm<sup>2</sup>. Precise guide rail (accurate to the  $\mu$ m) made sure that the distance between light and sample base was 34m and detector was 8m. In the process of measurement, electron in the synchrotron radiation storage ring radiated high-energy X-ray when the magnetic field steers. Being adjusted to 55keV after a series of processing, electrons penetrated the front of injector and exposure to scintillation crystal, turned into ordinary visible light and captured the X-ray absorption image at the front of injector by CCD camera. Injector rotated 180° at the speed of 1.8°/s on the sample rotation stage. During rotation, CCD camera captured an X-ray absorption image every 0.2° with 10s exposure time and 9mm spatial resolution of the image.

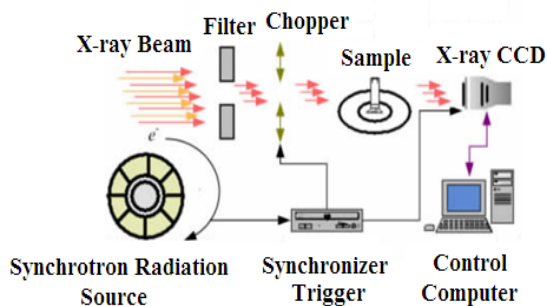


**Figure 1** Test bench and the main equipment

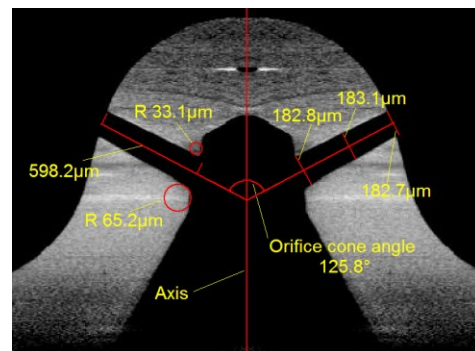


**Figure 2** Measurement of orifice diameters, orifice length, orifice angle and orifice inlet curvature

As shown in figure 2, the orifice top diameter is 182.8 $\mu$ m, the orifice middle diameter is 183.1 $\mu$ m and the orifice bottom diameter is 182.7 $\mu$ m. The orifice length is 598.2 $\mu$ m, the top and bottom orifice inlet curvature are 65.2 $\mu$ m and 33.1 $\mu$ m. The orifice cone angle is 125.8°. This injector structure was the basis of the consequent nozzle flow and spray simulation.

## Spray Simulation Coupled with Nozzle Flow

### Nozzle flow model

The nozzle flow was modelled with two-fluid model. In two-fluid models, the liquid and vapor phases are treated separately using two sets of conservation equations. The model is based on the transport of volume fraction, and a source term representing phase transition that is governed by the difference between local pressure and vapour pressure. Cavitation is assumed to occur due to the presence of bubble nuclei or micro bubbles within the liquid, which can grow or collapse, as described by the vapor fraction transport equation. The growth and collapse of the bubble are taken into account according to the Rayleigh's simplified bubble dynamics equation<sup>[12]</sup>.

It is assumed that all vapor bubbles in a control volume have the same radius and a homogenous distribution. This assumption allows us to describe the bubble distribution by a single scalar field, the vapor volume fraction  $\alpha_v$ . Assuming that only one liquid phase and the corresponding liquid-vapor phase can occupy the control volume where cavitation takes place, equation(1) gives a relationship between the vapor volume fraction  $\alpha_v$  and the average vapor bubble radius  $R$ :

$$\alpha_v = \frac{V_v}{V} = \frac{N_{bub} \frac{4}{3} \pi R^3}{V_l + V_v} = \frac{n_0 V_l \frac{4}{3} \pi R^3}{V_l + n_0 V_l \frac{4}{3} \pi R^3} = \frac{n_0 \frac{4}{3} \pi R^3}{1 + n_0 \frac{4}{3} \pi R^3} \quad (1)$$

where  $V_v$  is the volume occupied by the vapor,  $V$  the total control volume,  $V_l$  the volume occupied by the liquid and  $N_{bub}$  the number of vapor bubbles in the control volume.

The vapor volume fraction  $\alpha_v$  inside a control volume can change due to convective transport and bubble growth or collapse. The equation(2) describing the transport of  $\alpha_v$  assumes that the vapor density is much smaller than the liquid density and is given by:

$$\frac{d}{dt} \int_V \alpha_v dV + \int_S \alpha_v (v - v_s) \cdot da = \int_V \frac{n_0}{1 + n_0 \frac{4}{3} \pi R^3} \frac{d}{dt} \left( \frac{4}{3} \pi R^3 \right) dV \quad (2)$$

The modeling of cavitation bubble growth rate that appears on the right-hand side of equation(3), is based on the Lagrangian observation of a cloud of bubbles, and the conventional bubble dynamic (observation of a single bubble in an infinite stagnant liquid). This analysis results in the so-called extended Rayleigh-Plesset equation:

$$R \frac{d^2 R}{dt^2} + \frac{3}{2} \left( \frac{dR}{dt} \right)^2 = \frac{p_{sat} - p_\infty}{\rho_l} - \frac{2\sigma}{\rho_l R} - 4 \frac{\mu_l}{\rho_l R} \frac{dR}{dt} \quad (3)$$

where  $p_{sat}$  is the saturation pressure corresponding to the temperature at the bubble surface,  $p_\infty$  is the pressure of the surrounding liquid,  $\rho_l$  and  $\mu_l$  are the liquid density and viscosity, and  $\sigma$  is the surface tension coefficient.

The precise geometry structure of nozzle obtained by synchrotron radiation measurement was used to simulate the nozzle flow. Figure 3 was the structure used for nozzle flow simulation. All simulations were made with the standard  $k-\varepsilon$  turbulence model with standard wall functions. The solver was based on the pressure correction method and the SIMPLEc algorithm was used. The upwind differencing scheme was used for the discretization of the  $k-\varepsilon$  turbulence model equations. The cavitation model based on the Rayleigh equation links the rate of change of the bubble radius with the local pressure. In this model both the liquid and vapor density are constant and there is no slip between bubbles and liquid.

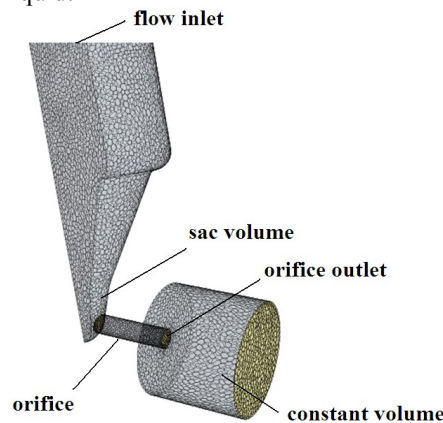


Figure 3 The mesh of nozzle used for calculation

### Spray model

The near-field dense spray was simulated with the VOF multiphase model. The atomization of diesel sprays is modeled as a turbulent mixing process of the liquid fuel with the ambient gas. At a certain downstream location, where the spray is diluted, this Eulerian spray approach was switched to conventional Lagrangian approach.

It was assumed that the spray zones, where the distance to orifice outlet is longer than 2mm, were dilute spray zone. The simulation cells of switch location cross-section, whose liquid volume of fraction was bigger than 0.5, were chosen as the fuel injector cells. The positions of these cells were considered as the position of the droplet parcels injected and the velocities of these cells were considered as the initial velocities (magnitude and direction) of droplets. So this model could simulate the spray angle and it was not needed to give previously. The initial droplet size was determined by the fuel liquid volume of fraction. The diameters of fuel droplets were proportional to the volume of fraction value of fuel liquid. It was assumed that the initial size was the orifice diameter multiply by corresponding scale factor<sup>[13]</sup>.

The conventional Lagrangian spray was simulated by STAR-CD. Theoretical studies provided a criterion for the onset of break-up and concurrently an estimate of the stable droplet diameter,  $D_{d,stable}$ , and the characteristic time scale  $\tau_b$  of the break-up process. This allows the break-up rate to be calculated from equation(4):

$$\frac{dD_d}{dt} = -\frac{(D_d - D_{d,stable})}{\tau_b} \quad (4)$$

Where  $D_d$  is the instantaneous droplet diameter.

Instability is determined by a critical value of the Weber number ( $We$ ) and the droplet Reynolds number ( $Re_d$ ), equation (5)(6):

$$We = \frac{\rho|u - u_d|^2 D_d}{2\sigma_d} \geq C_{b1} \quad (5)$$

$$Re_d = \frac{\rho|u - u_d| D_d}{\mu} \quad (6)$$

The criterion for the onset of this Stripping break-up regime is

$$\frac{We}{\sqrt{Re_d}} \geq C_{s1} \quad (7)$$

The characteristic time scale for this Stripping break-up regime is

$$\tau_b = \frac{C_{s2}}{2} \left( \frac{\rho_d}{\rho} \right)^{1/2} \frac{D_d}{|u - u_d|} \quad (8)$$

Here, the empirical coefficient  $C_{s1}$  is the value 0.5 and  $C_{s2}$  is in the range 2 to 20.

## Results and Discussion

### Injection pressure

The VOF value of liquid fuel and initial velocity (magnitude and direction) at switch position were two key parameters of the switch criteria. The VOF value was obtained by the nozzle flow simulation in switch position, as shown in figure 4. The  $i$ ,  $j$ , and  $k$  were the three directions of velocity. Velocity in  $k$  was the direction vertical to orifice outlet cross-section. The mean velocity in  $k$  increased with the growing of injection pressure from 10MPa to 100MPa, while the VOF value of liquid fuel decreased. The velocity in  $i$  and  $j$  direction were contributed to the spray angle.

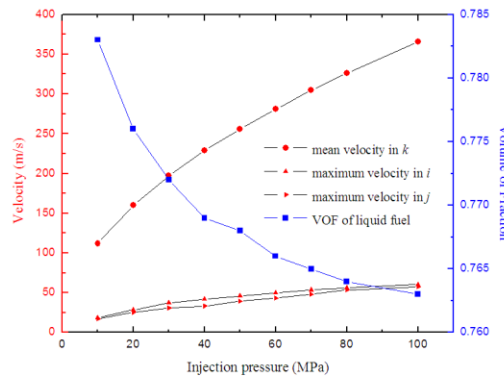
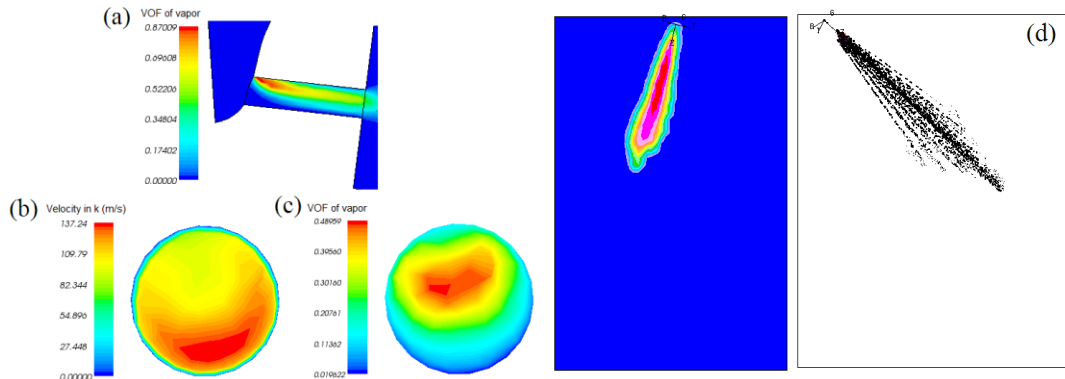
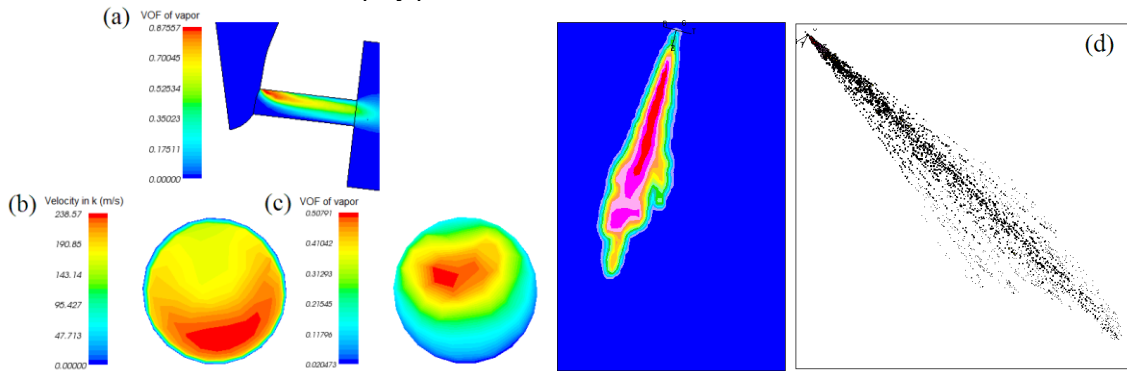


Figure 4 The velocity and VOF in different injection pressures (1ms)



**Figure 5** Injectoin pressure 10MPa: (a) volume of fraction of fuel vapor (cross-section), (b) velocity in k direction (vertical direction of orifice outlet), (c) volume of fraction of fuel vapor (orifice outlet), (d) mass fraction of fuel and spray particle distribution.



**Figure 6** Injectoin pressure 30MPa: (a) volume of fraction of fuel vapor (cross-section), (b) velocity in k direction (vertical direction of orifice outlet), (c) volume of fraction of fuel vapor (orifice outlet), (d) mass fraction of fuel and spray particle distribution.

As shown in figure 5 and figure 6, the structure of spray were asymmetric as the result of nozzle flow (cavitation and turbulence). The fuel liquid spray penetration of 10MPa was obviously shorter than that of 30MPa. The velocity in k in the cavitation zone was smaller than other zone. The cavitation zone in the nozzle was not asymmetric.

### Ambient gas pressure

The ambient gas density had a significantly larger effect on spray penetration and a smaller effect on spray dispersion. The different chamber pressures correspond to different ambient gas density. The injection pressure was 30MPa and the ambient gas pressure was 0.2MPa, 1MPa and 2MPa, respectively. As shown in figure 7, the spray penetration lengths under different ambient gas pressures were obviously different. The larger the ambient gas pressure, the shorter the penetration length.

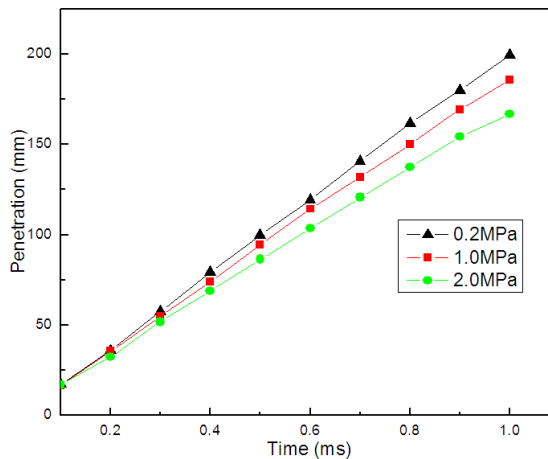


**Figure 7** spray penetration of different ambient gas pressure

**Validation**

The DLH1105 product engine was reconstructed, the optical system and the control and data acquisition system were developed to set up a set of visual engine for experiment of spray, as shown in figure8 (left). The visual spray experiment was performed on this bench and the spray development process were shown in figure8 (right).

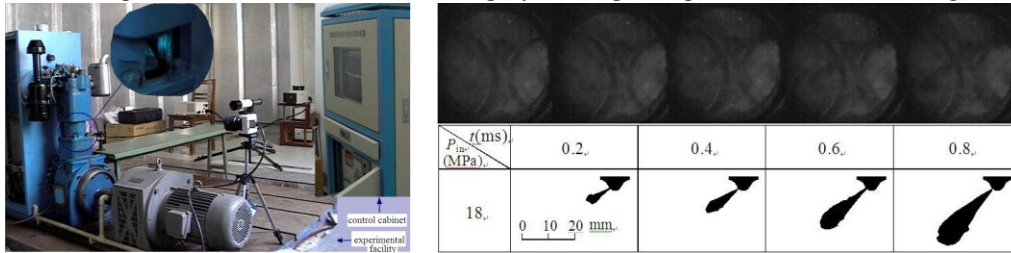


**Figure 8** left: visual engine for spray and combustion, right: experimental results of spray

From figure 9, it can be easily found that the simulation data of coupling spray was much closer to the experimental data than that without consideration of the detailed nozzle cavitating flow.

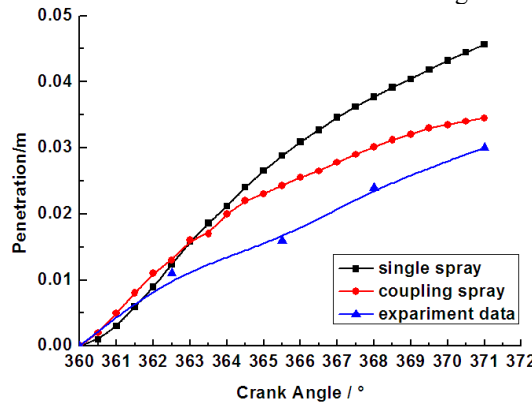


**Figure 9** Tip penetrations of single spray, coupling spray and experiment data

**Effect of different injector geometries on the spray characteristics**

Using above verified coupling spray model, the multi-scheme numerical simulations were carried out for different nozzle geometry parameters, such as the ratio of nozzle hole length to diameter( $l/d$ ), hole entrance curvature radius( $r$ ) and three different nozzle configurations like Sac-hole, IMPROVED and VCO type of nozzle to analyze the effect of nozzle geometries on the subsequent spray structure.

**The ratio of nozzle hole length to diameter.** The nozzle configuration was Sac-hole. The pressure at the inlet was 50MPa and the back pressure was 0.5MPa. The hole entrance curvature radius was 0. The simulation results for different ratios of nozzle hole length to diameter ( $l/d=2, 3$  and 4) were shown in figure 10. The vapor volume fraction at the hole outlet and the spray tip penetration decreased while Sauter Mean Diameter-SMD increases if the ratio of length to diameter increased.

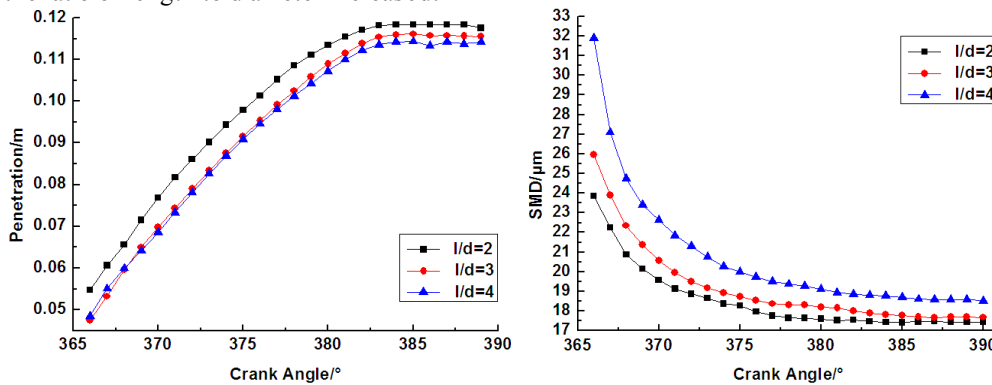


**Figure 10** Spray tip penetration and SMD for  $r/d=2, 3$  and 4

**The hole entrance curvature radius.** The nozzle configuration was Sac-hole. The pressure at the inlet was 50MPa and the back pressure was 0.5MPa. The ratio of hole length to diameter was 4. Figure 11 showed the simulation results for different hole entrance curvature radius( $r=0, r=0.0228\text{mm}$  and  $r=0.0456\text{mm}$ ) of the nozzle.

It presented that the hole entrance curvature radius had a strong effect on volume fraction of vapor distribution. If the ratio of hole length to diameter decreased, the vapor volume fraction at the hole outlet and the spray tip penetration decreased rapidly and the place where cavitation appeared became further away from the hole entrance.

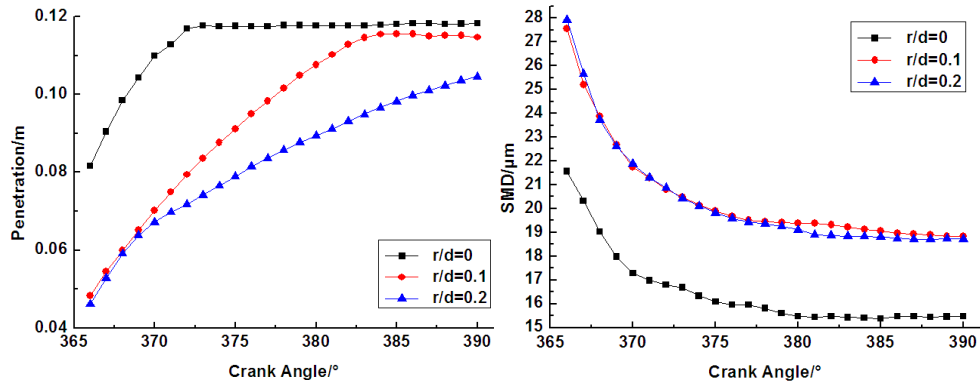


Figure 11 Spray tip penetration and SMD for  $r=0, 0.0228$  and  $0.0456$ mm

**Three types of nozzle with different sac volume.** The different sac geometries were considered here. The standard nozzle (STD) had a larger sac volume before the nozzle holes. The VCO (Valve Closed Orifice) nozzle has nearly no sac volume and the fuel enters the holes across the narrow annulus of nozzle. While the improved nozzle had a sac volume much smaller than the STD nozzle and the upward location of the nozzle hole similar with the VCO nozzle.

For these three different models, they had the same boundary conditions and orifice geometry. Inlet pressure was 50MPa and the back pressure was 0.5MPa. The calculation results were shown in Figure 12. Sac-hole nozzle had the shortest spray tip penetration and the largest value of SMD, while VCO nozzle had the longest penetration and smallest value of SMD. Considering of nozzle cavitating flow comprehensively, from the aspect of spray tip penetration and SMD, IMPROVED nozzle could acquire better spray characteristics.

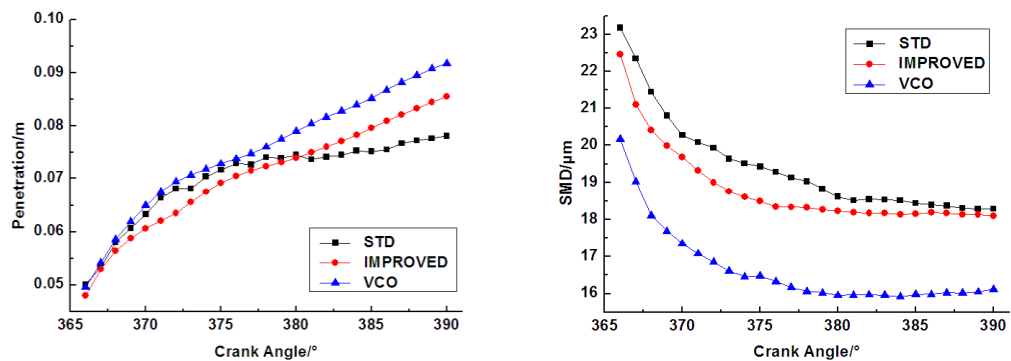


Figure 12 Spray tip penetration and SMD of three different types of nozzle

## Summary and Conclusions

The X-ray phase contrast imaging measurement could obtain a high-precision three-dimensional structure model of nozzle internal geometry. It was helpful to establish the CFD model of nozzle more exactly. Comparing the visual spray experiment data and numerical results, it was verified that the spray model coupled with cavitating flow in nozzles was more accurate than the normal spray model widely used nowadays. The multi-scheme numerical simulations indicate that the nozzle structure has a strong effect on internal cavitating flow and subsequent spray. The simulation results supply the theoretical foundation for the optimization design of the injector.

At present, the initial parcel size in the simulation was given by empirical formula. In our future work, we plan to simulate the initial parcel size by the liquid mass fraction and the liquid surface density (liquid surface area per unit volume) transport equations<sup>[14]</sup>.

## Acknowledgements

This research was supported by the National Natural Science Foundation of China (No. 51176066, No.51076060), Jiangsu province industry support plan (No. BE2010198) and A Project Funded by the Priority Academic Program Development of Jiangsu Higher Education Institutions. This research was also supported by the SSRF (Synchrotrons of Shanghai Synchrotron Radiation Facility).

## References

- [1] Wei Ning and Rolf D. Reitz, *International Multidimensional Engine Modeling User's Group Meeting, Detroit, MI, April 2007*
- [2] S.Som and S.K.Aggarwal, *Journal of Engineering for Gas Turbines and Power*, 132:042802-1-12(2010).
- [3] F. Payri, V. Bermudez, R. Payri, F.J. Salvador., *Fuel*, 2004, 83:419-431.
- [4] X. Jiang a,b, G.A. Siamas, K. Jagus, T.G. Karayiannis., *Progress in Energy and Combustion Science*, 2010, 26: 131-167.
- [5] HE xia, YUAN Jianping, LI De tao, LIANG Feng biao., *Chinese Internal Combustion Engine Engineering*, 2005, 26(6): 19-21.
- [6] YUJIE WANG and JIN WANG, *Nature Physics*, 2008, 4(4):305-309.
- [7] Reitz, R. D. *Atomization and Sprays*, Vol. 3(4), 1987:309-337.
- [8] Vallet, A., Burluka, A. A., Borghi, R., *Atomization and Sprays*, Vol. 11 (6), 2001:192-236.
- [9] Som, S. and Aggarwal, S. K., *Atomization and Sprays*, Vol. 19 (9), 2009:885-903.
- [10] J.Shinjo and A. Umemura., *International Journal of Multiphase Flow*, 36(2010):513-532.
- [11] Haohu LI and Xiaohan XU., *Modern Physics*, 2010, 22(3):14-19.
- [12] Martynov, S., *Ph.D. thesis, University of Brighton*, Brighton, 2005.
- [13] Reitz, R.D. and Diwakar, R., *SAE Paper*, 870598, 1987.
- [14] Yue Wang, Won Geun Lee and Rolf Reitz., *SAE Paper*, 2011-01-0386.